

Non-Spherical Shapes of the Proton: Existence, Measurement and Computation

Gerald A. Miller

University of Washington Seattle, WA 98195-1560

Introduction How can the spin 1/2 object known as the proton have a non-spherical shape? Why would a physicist even think of such a concept? Can a non-sphericity (or pretzelosity) be measured or computed? This note is concerned with such questions.

The notion that the proton might not have a spherical shape has its impetus in the discovery that the spins of quarks and anti-quarks account for only about 30% of the total angular momentum [1]. Many experiments have sought the origins of the remainder, expected to arise from quark and gluon orbital angular momentum or from pairs of strange quarks.

This article is concerned with the relation between the quark orbital angular momentum and the non-spherical shape of the proton. A number of concerns arise immediately. As a particle of spin 1/2, the proton can have no quadrupole moment, according to the Wigner-Eckart theorem. In elastic electron-proton scattering experiments, the effects of relativity cause the initial and final wave functions to differ because their momenta differ. For example, one thinks of a particle in relativistic motion having a pancake shape because of the effects of Lorentz contraction. Such an effect is not a manifestation of the intrinsic proton shape.

The presence of significant orbital angular momentum can only lead to a non-spherical shape if such can be defined by an appropriate operator. We used the proton model of Ref. [2]-[4] to show [5] that the rest-frame ground-state matrix elements of spin-dependent density operators reveal a host of non-spherical shapes.

Experimental genesis The electromagnetic current matrix element can be written in terms of the Dirac $F_1(Q^2)$ and Pauli $F_2(Q^2)$ form factors, Q^2 is the negative of the square of the space-like four-momentum transfer. These form factors are probability amplitudes that the proton can absorb a squared four momentum transfer Q^2 and still remain a proton. Two exist because the rapidly moving quarks within the proton carry both charge and magnetization densities. For $Q^2 = 0$ the form factors F_1 and κF_2 are the charge and the anomalous magnetic moment κ in units e and $e/2M_N$, and the magnetic moment $\mu = 1 + \kappa$. The Sachs form factors are

$$G_E = F_1 - \frac{Q^2}{4M_N^2} \kappa F_2, G_M = F_1 + \kappa F_2.$$

In the non-relativistic quark model, G_E and G_M are Fourier transforms of the ground state matrix elements of the quark charge ($\sum_{i=1,3} e_i \delta(\mathbf{r} - \mathbf{r}_i)$) and magnetization $\sum_{i=1,3} \frac{e_i}{2m_i} \delta(\mathbf{r} - \mathbf{r}_i)$ density operators. Thus, non-relativistically, one expects that $G_E(Q^2)/\mu G_M(Q^2) = 1$. Interestingly, the opposite highly relativistic limit, in which dimensional counting applies, predicted [6] (using the notion of helicity conservation in the interactions between photons and massless fermions) that $\lim_{Q^2 \rightarrow \infty} QF_2/F_1 = m_q/Q^2$, where m_q is the small mass of a down or up quark. This is equivalent to the non-relativistic expectation. Thus theoretical expectations (and early data) were that the ratio of the Sachs form factors would be constant. These expectations were dramatically thrown aside with the discovery that G_E/G_M falls rapidly with increasing values of Q^2 and that QF_2/F_1 is approximately constant [7], [8]. See Fig. 1 which also displays the results of our 1995 theory [2, 3].

An explanation [3] of how the model of [2] describes the data showed that the constant ratio QF_2/F_1 emerges from the model's relativistic aspects. For the proton wave function, only the component in which the first two quarks have a vanishing total angular momentum enters in computing the electromagnetic form factors. Then the angular momentum of the proton S is governed by that of the third quark. The relevant Dirac spinor is:

$$u(\mathbf{K}, S) = \frac{1}{\sqrt{E(K) + m_q}} \begin{pmatrix} (E(K) + m_q)|S\rangle \\ \boldsymbol{\sigma} \cdot \mathbf{K}|S\rangle \end{pmatrix}, \quad (1)$$

with $E(K) = (K^2 + m_q^2)^{1/2}$. The magnetic quantum number of the proton is denoted by S , and the lower component contains a term $\boldsymbol{\sigma} \cdot \mathbf{K}$ that allows the quark to have a spin opposite to that of the proton's total angular momentum. The vector \mathbf{K} reveals the presence of the quark orbital angular momentum: the struck quark may carry a spin that is opposite to that of the proton. Consequently nucleon helicity [9] is not conserved [10, 11].

Spin-dependent density operators We interpret orbital angular momentum in terms of the shapes of the proton by these are exhibited through the rest-frame

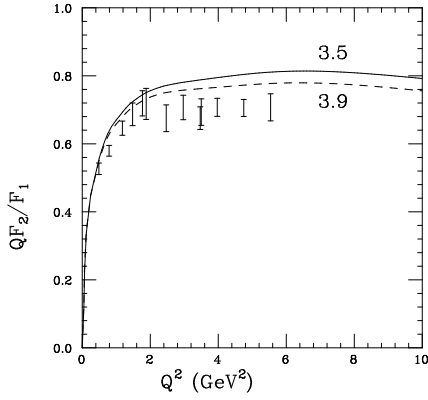


FIG. 1: The ratio QF_2/F_1 . The curves from the 1995 theory of [2] for the ratio are labeled by the value of a model parameter. The data are from [7] and [8]. Figure reprinted with permission from [3]. Copyright 2002 by the American Physical Society.

ground-state matrix elements of spin-dependent density operators [5]. The usual quantum mechanical density operator is $\hat{\rho}(\mathbf{r}) = \sum_i \delta(\mathbf{r} - \mathbf{r}_i)$, where \mathbf{r}_i is the position operator of the i 'th particle; but for particles of spin 1/2 one can measure the *combined* probability that particle is at a given position \mathbf{r} and has a spin in an arbitrary, fixed direction specified by a unit vector \mathbf{n} . The resulting spin-dependent density SDD operator is

$$\hat{\rho}(\mathbf{r}, \mathbf{n}) = \sum_i \delta(\mathbf{r} - \mathbf{r}_i) \frac{1}{2} (1 + \boldsymbol{\sigma}_i \cdot \mathbf{n}). \quad (2)$$

To understand the connection between the spin-dependent density and orbital angular momentum, consider a first example of a single charged particle moving in a fixed, rotationally-invariant potential in an energy eigenstate $|\Psi_{1,1,1/2,s}\rangle$ of quantum numbers: $l = 1, j = 1/2$, polarized in the direction $\hat{\mathbf{s}}$ and radial wave function $R(r_p)$. The wave function can be written as $(\mathbf{r}_p | \Psi_{1,1,1/2,s} \rangle = R(r_p) \boldsymbol{\sigma} \cdot \hat{\mathbf{r}}_p | s \rangle$. The ordinary density, $\rho(r) = \langle \Psi_{1,1,1/2,s} | \delta(\mathbf{r} - \mathbf{r}_p) | \Psi_{1,1,1/2,s} \rangle = R^2(r)$, a spherically symmetric result because the effects of the Pauli spin operator square to unity. But the matrix element of the SDD is more interesting:

$$\rho(\mathbf{r}, \mathbf{n}) = \frac{R^2(r)}{2} \langle \hat{\mathbf{s}} | \boldsymbol{\sigma} \cdot \hat{\mathbf{r}} (1 + \boldsymbol{\sigma} \cdot \hat{\mathbf{n}}) \boldsymbol{\sigma} \cdot \hat{\mathbf{r}} | \hat{\mathbf{s}} \rangle. \quad (3)$$

The magnetic quantum defines an axis, \mathbf{s} and the direction of vectors can be represented in terms of this axis: $\hat{\mathbf{s}} \cdot \hat{\mathbf{r}} = \cos \theta$. Suppose $\hat{\mathbf{n}}$ is either parallel or anti-parallel to the direction of the proton angular momentum vector $\hat{\mathbf{s}}$. Then $\rho(\mathbf{r}, \mathbf{n} = \hat{\mathbf{s}}) = R^2(r) \cos^2 \theta$, $\rho(\mathbf{r}, \mathbf{n} = -\hat{\mathbf{s}}) = R^2(r) \sin^2 \theta$, and the non-spherical shape is exhibited. The average of these two cases is a spherical shape.

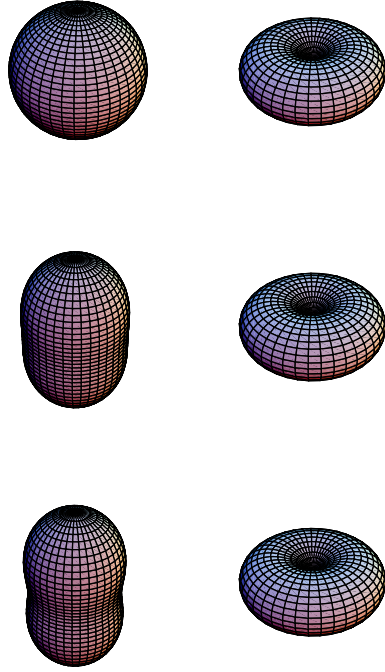


FIG. 2: (Color online) Shapes of the proton. \mathbf{S} is in the vertical direction. Left column quark spin parallel to nucleon spin. Right column : quark spin anti-parallel to nucleon spin. The value of K increases from 0 to 1 to 4 GeV/c. Figure reprinted with permission from [5]. Copyright 2003 by the American Physical Society.

Another useful example is that of the Dirac four-component spinor electron wave function of the hydrogen atom ground state, with relative size of the lower component governed by the fine structure constant, α . The expectation value of the spin-dependent density operator, computed using Dirac matrices, with $\boldsymbol{\sigma} = \gamma^0 \boldsymbol{\gamma} \cdot \mathbf{n}$, is $\rho(\mathbf{r}, \hat{\mathbf{n}} = \hat{\mathbf{s}}) \propto [1 + \alpha^2/4 \cos^2 \theta] \sim 1 + 10^{-5} \cos^2 \theta$ with $\mathbf{n} = \hat{\mathbf{s}}$. For $\mathbf{n} = -\hat{\mathbf{s}}$, $\rho(\mathbf{r}, \hat{\mathbf{n}} = -\hat{\mathbf{s}}) = \alpha^2 \sin^2 \theta/4$. Relativity as manifest by lower components of the Dirac wave function causes the hydrogen atom to be slightly, but definitely, non-spherical!

The notion of the SDD can be extended. In condensed matter applications [13] neutrons interact with atomic electrons, and only the (electronic) spin-dependent term of Eq. (2) is used. For quark systems, the densities could be weighted by the charge or flavor of the quarks, or use other operators. In particular, we use [12]

$$\hat{\rho}_R(\mathbf{r}, \mathbf{n}) \equiv \sum_i \delta(\mathbf{r} - \mathbf{r}_i) \frac{1}{2} (1 + \gamma_i^0 \boldsymbol{\sigma}_i \cdot \mathbf{n}), \quad (4)$$

which is more experimentally accessible.

Now turn to the proton. Its wave function is specified in momentum space, so we define [5] a charge-weighted

SDD operator (the probability that a quark has a momentum \mathbf{K} and spin direction \mathbf{n}):

$$\hat{\rho}(\mathbf{K}, \mathbf{n}) = \int \frac{d^3\xi}{(2\pi)^3} e^{i\mathbf{K}\cdot\boldsymbol{\xi}} \bar{\psi}(\boldsymbol{\xi}) \frac{\hat{Q}}{e} (\gamma^0 + \boldsymbol{\gamma} \cdot \mathbf{n} \gamma_5) \psi(\mathbf{0}), \quad (5)$$

where \hat{Q}/e is the quark charge operator in units of the proton charge. The quark field operators are evaluated at equal time, $\xi^0 = 0$. For the case of $\hat{\rho}_R$ the term $\boldsymbol{\gamma} \cdot \mathbf{n}$ is replaced by $\gamma^0 \boldsymbol{\gamma} \cdot \mathbf{n}$. For a spin-polarized (in the $\hat{\mathbf{S}}$ direction) proton at rest $|\Psi_S\rangle$, the matrix elements of $\hat{\rho}$, $\hat{\rho}_R$ (SDDs) are given by

$$\begin{aligned} \rho(\mathbf{K}, \mathbf{n}, \mathbf{S}) &= A + B\mathbf{n} \cdot \hat{\mathbf{S}} + C(\mathbf{n} \cdot \hat{\mathbf{K}} \hat{\mathbf{S}} \cdot \hat{\mathbf{K}} - \frac{1}{3}\mathbf{n} \cdot \hat{\mathbf{S}}) \\ \rho_R(\mathbf{K}, \mathbf{n}, \mathbf{S}) &= A_R + B_R\mathbf{n} \cdot \hat{\mathbf{S}} \\ &+ C_R(\mathbf{n} \cdot \hat{\mathbf{K}} \hat{\mathbf{S}} \cdot \hat{\mathbf{K}} - \frac{1}{3}\mathbf{n} \cdot \hat{\mathbf{S}}), \end{aligned} \quad (6)$$

where A, B, \dots are scalar coefficients. These forms represent the most general *rest frame* shape of the proton, if parity and rotational invariance are upheld [5].

We display the shapes of $\rho(\mathbf{K}, \mathbf{n}, \mathbf{S})$ [5] in Fig. 2 for the cases of quark spin parallel and anti-parallel to the polarization direction of the proton \mathbf{S} . The shape for a given value of K is determined by the ratio of the upper to lower components of the quark Dirac spinor Eq. (1). The relatively large value of the ratio implies considerable non-sphericity and a sharp contrast between the proton and hydrogen atom. As the value of K increases from 0 to 4 GeV/c the shape varies from that of a sphere to that of a peanut, if $\mathbf{n} \parallel \mathbf{S}$. The torus or bagel shape is obtained if $-\mathbf{n} \parallel \mathbf{S}$. Taking $\mathbf{n} \perp \mathbf{S}$ leads to some very unusual shapes shown in Fig. 3. Using the given model [5], one may also obtain in coordinate space SDDs. Possible shapes include a pretzel form [5].

Any wave function yielding a non-zero value of the coefficient $C(\mathbf{K}^2)$ or $C_R(\mathbf{K}^2)$ represents a system of a

non-spherical shape. If the relativistic constituent quark model of [2] is used, the extra γ^0 changes the sign of the lower component of the wave function, causing $C_R = -C$. Thus either C_R or C can be used to infer information about the possible shapes of the nucleon. Measuring either would require controlling the three different vectors \mathbf{n}, \mathbf{S} and \mathbf{K} .

A specific aspect of $\hat{\rho}(\mathbf{K}, \mathbf{n})$ is easily related to completed experiments because $\int d^3K \hat{\rho}(\mathbf{K}, \mathbf{n})$ is a local operator. Its matrix element is a linear combination of the charge, integrals of spin-dependent structure functions Δq (quark contribution to the proton total angular momentum), and g_A that can be determined from previous measurements. We find

$$\begin{aligned} &\int d^3K \langle N | \hat{\rho}(\mathbf{K}, \mathbf{n} = \hat{\mathbf{S}}, \mathbf{S}) - \hat{\rho}(\mathbf{K}, \mathbf{n} = -\hat{\mathbf{S}}, \mathbf{S}) | N \rangle \\ &= \frac{1}{6}(\Delta q + \frac{1}{2}g_A) = 0.68, \end{aligned} \quad (7)$$

in which $\Delta q = 0.3$ [1] and $g_A = 1.26$. The model we use gives 0.74 for the above quantity, indicating that shapes discussed here may not be unrealistic.

Measuring the Non-Spherical Shape of the Nucleon Can non-spherical shapes be measured? While measurements of the matrix elements of the non-relativistic spin-density operator [13] reveal highly non-spherical densities, finding the non-spherical nature of the proton has remained a challenge. Here we explain how matrix elements of the spin-dependent density may be measured using their close connection with transverse momentum dependent parton densities.

The densities of Eq. (6) require that the system be probed with identical initial and final states. But this condition also enters in measurements of both ordinary and transverse-momentum-dependent TMD parton distributions. The latter [14] are:

$$\Phi^{[\Gamma]}(x, \mathbf{K}_T) = \int \frac{d\xi^- d^2\xi_T}{2(2\pi)^3} e^{iK \cdot \xi} \langle P, S | \bar{\psi}(0) \Gamma \mathcal{L}(0, \xi; n_-) \psi(\xi) | P, S \rangle \Big|_{\xi^+=0}, \quad (8)$$

where the specific path n^- is that of Appendix B of [14]. The functions $\Phi^{[\Gamma]}$ depend on the fractional momentum $x = K^+/P^+$, \mathbf{K}_T and on the hadron momentum P . The

operator Γ can be any Dirac operator, *e.g.* $\Gamma = i\sigma^{i+} \approx \sqrt{2}\gamma^0\gamma^i\gamma^5$, related to h_{1T}^\perp , which causes the non-spherical nature of $\hat{\rho}_R$.

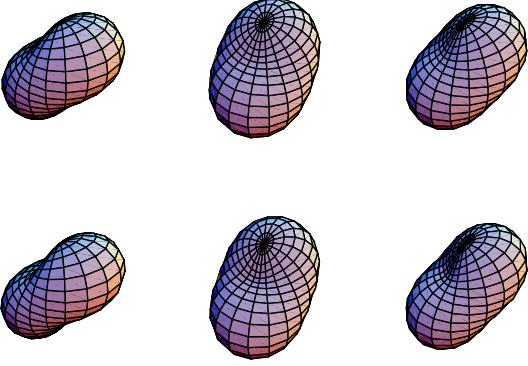


FIG. 3: Shapes of the proton with $\mathbf{n} \cdot \mathbf{s} = 0$. Left column, \mathbf{n} points (out of page), central: \mathbf{n} points sideways, right \mathbf{n} is out of the page at a 45° angle. The momentum K increases from 1 to 4 GeV/c. Figure reprinted with permission from [5]. Copyright 2003 by the American Physical Society.

It is therefore tempting to try to associate an SDD such as that of Eq. (5) with TMDs, but one difference is essential. Parton density operators Eq. (8) depend on quark-field operators defined at a fixed light cone time $\xi^+ = \xi^3 + \xi^0 = 0$ while our SDD is an equal-time, $\xi^0 = 0$, correlation function. However, a relation between the two sets of operators is obtained [12] by integrating the TMD over all values of x setting ξ^- to zero, and integrating Eq. (5) over all values of K_z so that $\xi^3 = 0$. After integration, $\xi^\pm = 0$ for both functions. The density operators, derived from those of Eq. (6) are denoted by adding a T to the subscript. Thus $\hat{\rho}_{RT}(\mathbf{K}_T, \mathbf{n}) \equiv \int_{-\infty}^{\infty} dK_z \hat{\rho}_R(\mathbf{K}, \mathbf{n})$. It is therefore a matter of algebra to show that

$$\rho_{RT}(\mathbf{K}_T, \mathbf{n}_T, \mathbf{S}_T)/M = \tilde{f}_1(K_T^2) + \tilde{h}_1(K_T^2) \mathbf{n} \cdot \hat{\mathbf{S}}_T + \frac{(\hat{\mathbf{n}}_T \cdot \mathbf{K}_T \hat{\mathbf{S}}_T \cdot \mathbf{K}_T - \frac{1}{2} K_T^2 \hat{\mathbf{n}} \cdot \hat{\mathbf{S}}_T)}{M^2} \tilde{h}_{1T}^\perp(K_T^2), \quad (9)$$

in the rest frame, where a tilde is placed over each TMD parton distribution to denote an x -integrated function. Finding that non-zero value of $\tilde{h}_{1T}^\perp \neq 0$ would demonstrate that the proton is not spherical.

The term \tilde{h}_{1T}^\perp causes distinctive experimental signatures in semi-inclusive lepton production hadron production experiments [15, 16]. If the target is polarized in a direction \mathbf{S}_T transverse to the lepton scattering plane, the cross section acquires a term proportional to $\cos(3\phi_h^l)$ where ϕ_h^l is the angle between the hadron production plane (defined by the momenta of the incoming virtual photon and the outgoing hadron) and the lepton scattering plane. A similar effect occurs in electroweak semi-inclusive deep inelastic lepton production [17]. In each of these cases, the momentum of the virtual photon and its vector nature provide the analogue of the vector \mathbf{n} needed

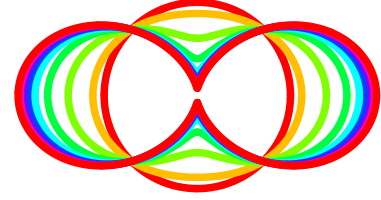


FIG. 4: Transverse shapes of the proton; $\sqrt{2} \hat{\rho}_{RT}(\mathbf{K}_T, \mathbf{n}) / \tilde{f}_1(K_T^2)$. The horizontal axis is the the direction of \mathbf{S}_T and $\mathbf{n} = \hat{\mathbf{S}}_T$, $\phi_n = \pi$. The shapes vary from circular to highly deformed as K_T is increased from 0 to 2.0 GeV in steps of 0.25 GeV. Figure reprinted with permission from [12]. Copyright 2007 by the American Physical Society.

to define the spin-dependent density. The hadronic transverse momentum provides the third, \mathbf{K}_T . Another possibility occurs in the Drell-Yan reaction $pp(\uparrow) \rightarrow l\bar{l}X$, using one transversely polarized proton [18].

The shapes inherent in Eq. (9) are illustrated using the spectator model of [19]. Here ϕ is the angle between \mathbf{K}_T and \mathbf{S}_T and ϕ_n is the angle between \mathbf{n} and \mathbf{S}_T . The transverse shapes of the proton (assuming a struck u quark) are shown in Fig. 4, taking $\phi_n = \pi$. This emphasizes the non-spherical nature because the first two terms of Eq. (9) tend to cancel. The shapes of Eq. (9) can be thought of as projections of the shapes displayed in previous figures.

The model [19] indicates that the functions f_1, h_1 and h_{1T}^\perp have very similar x dependence, so that measurements at values of x for which these functions peak should be sufficient to construct the required integrals over x .

The non-spherical nature of the nucleon shape is determined by the non-vanishing of the TMD h_{1T}^\perp . It is very exciting that experiments planned at Jefferson Laboratory aim to specifically measure h_{1T}^\perp [20] and therefore determine whether or not the proton is round.

Connection with lattice QCD The non-spherical shape of the nucleon can be established in lattice QCD by computing the lattice version of the angular integral of the matrix element:

$$F_\Gamma(r) = \int d\hat{\mathbf{r}} Y_{20}(\hat{\mathbf{r}}) \langle \Psi_S | \bar{\psi}(\mathbf{r}) (\gamma^0 + \Gamma \boldsymbol{\gamma} \cdot \mathbf{n} \gamma_5) \psi(\mathbf{0}) | \Psi_S \rangle$$

where $\Gamma = 1$ or γ^0 and the link operator is not displayed.

A non-zero value of $F(r)$ for any value of r would immediately tell us that the proton does not have a spherical shape. Matrix elements of $\bar{\psi}_\alpha(\mathbf{r})\psi_\beta(\mathbf{0})$ have been evaluated for the case when the separation is one or two links. Thus the relevant information is available. Preliminary results for $F_T(\mathbf{r})$ exist only for separations of one-link, and current statistics are not high [21]. Another possibility, closely related to finding h_{1T}^\perp , would be to take the spatial component of \mathbf{r} to be perpendicular to \mathbf{s} and integrate over the transverse directions. I hope that the lattice QCD community will find it of sufficient interest to warrant the effort of a detailed, high-statistics calculation.

Summary The nature of the proton wave function can be elucidated by studying the matrix elements of a generalized density operator. Spin-dependent quark densities SDD are defined as matrix elements of density operators in proton states of definite spin-polarization, and shown to have an infinite variety of non-spherical shapes. For

high momentum quarks with spin parallel to that of the proton, the shape resembles that of a peanut, but for quarks with anti-parallel spin the shape is that of a bagel. The matrix elements of the SDDs are closely related to specific transverse momentum dependent TMD parton distributions accessible in the angular dependence of the semi-inclusive processes $ep \rightarrow e\pi X$ and the Drell-Yan reaction $pp \rightarrow l\bar{l}X$. New measurements or analyses would allow the direct exhibition of the non-spherical nature of the proton. The TMDs can be computed using lattice QCD so that the non-spherical shapes could be measured experimentally and computed using fundamental theory.

Acknowledgments I thank the USDOE for partial support of this work. I thank C. Glasshauser and J. Ralston for emphasizing the importance of understanding the shape of the proton and H. Avakian, D. Boer, M. Burkardt, W. Detmold, L. Gamberg, K. Hafidi, A. Kvinikhidze, J.W. Negele, and J.C. Peng for useful discussions.

-
- [1] See e.g. E. W. Hughes and R. Voss, *Ann. Rev. Nucl. Part. Sci.* **49**, 303 (1999).
 - [2] M.R. Frank, B.K. Jennings and G.A. Miller, *Phys. Rev. C* **54**, 920 (1996).
 - [3] G. A. Miller and M. R. Frank, *Phys. Rev. C* **65**, 065205 (2002)
 - [4] G. A. Miller, *Phys. Rev. C* **66**, 032201 (2002).
 - [5] G. A. Miller, *Phys. Rev. C* **68**, 022201 (R) (2003), A. Kvinikhidze and G. A. Miller, *Phys. Rev. C* **73**, 065203 (2006).
 - [6] S. J. Brodsky and G. R. Farrar, *Phys. Rev. Lett.* **31**, 1153 (1973).
 - [7] M. K. Jones *et al.* *Phys. Rev. Lett.* **84**, 1398 (2000)
 - [8] O. Gayou *et al.* *Phys. Rev. Lett.* **88**, 092301 (2002)
 - [9] The ratio of QF_2/F_1 is a ratio of a helicity-changing to a helicity preserving matrix element.
 - [10] T. Gousset, B. Pire and J. P. Ralston, *Phys. Rev. D* **53**, 1202 (1996)
 - [11] V. M. Braun, A. Lenz, N. Mahnke and E. Stein, *Phys. Rev. D* **65**, 074011 (2002).
 - [12] G. A. Miller, *Phys. Rev. C* **76**, 065209 (2007).
 - [13] K. Prokeš *et al.* *Phys. Rev. B* **65**, 144429 (2002)
 - [14] P. J. Mulders and R. D. Tangerman, *Nucl. Phys. B* **461**, 197 (1996) [Erratum-*ibid.* **B 484**, 538 (1997)].
 - [15] D. Boer and P. J. Mulders, *Phys. Rev. D* **57**, 5780 (1998)
 - [16] A. Bacchetta and P. J. Mulders, *Phys. Rev. D* **62**, 114004 (2000).
 - [17] D. Boer, R. Jakob and P. J. Mulders, *Nucl. Phys. B* **564**, 471 (2000).
 - [18] D. Boer, *Phys. Rev. D* **60**, 014012 (1999)
 - [19] R. Jakob, P. J. Mulders and J. Rodrigues, *Nucl. Phys. A* **626**, 937 (1997).
 - [20] H. Avakian, *et al.* “Transverse Polarization Effects in Hard Scattering at CLAS12 Jefferson Laboratory”, LOI12-06-108, and private communication.
 - [21] H-W Lin, private communication.